Supermodes of Chiral Photonic Filters with Combined Twist and Layer Defects

Ian J. Hodgkinson,* Qi hong Wu,† Lakshman De Silva,‡ and Matthew Arnold§
Department of Physics, University of Otago, P.O. Box 56, Dunedin, New Zealand

Martin W. McCall‖
Department of Physics, The Blackett Laboratory, Imperial College of Science, Technology and Medicine, Prince Consort Road, London SW7 2BW, United Kingdom

Akhlesh Lakhtakia¶
Department of Engineering Science & Mechanics, Pennsylvania State University, University Park, Pennsylvania 16802-6812, USA
(Received 6 August 2003; published 26 November 2003)

We consider the circularly polarized localized modes of chiral photonic structures with combined central twist and isotropic layer defects. The general filter is shown to suffer from anomalous remittance and saturation of linewidth as the thickness of the structure is increased. However, by choosing parameters that phase match the elements of the round-trip matrix of the isotropic layer defect, we demonstrate the existence of supermodes that maintain exceptional purity of polarization state and exponential decrease in linewidth as the thickness is increased.

DOI: 10.1103/PhysRevLett.91.223903 PACS numbers: 42.25.Fx, 42.40.Eq, 42.79.Dj, 77.55.+f

Advances in the theory of chiral filters (CFs) and in the fabrication of sculptured thin films [1] (STFs) together offer promise for the realization of inorganic chiral photonic band gap structures, similar to those reported for cholesteric liquid crystals [2,3]. STFs are deposited layer by layer by physical vapor deposition and a key advantage is that layer and twist defects can be nanoengineered with precision. In recent years, STF technology has been used to fabricate an inorganic chiral photonic filter with a central layer defect [4] and a spacerless version with a central twist defect [5]. We now know, however, that these designs suffer from inherent constraints on polarization state and linewidth as discussed by Kopp and Genack for the spacerless filter [6], and from the effects of material absorbance as reported by Wang and Lakhtakia [7] for slanted chiral STFs. In this Letter, we consider the resonant modes of nondissipative chiral filters that have both a layer defect and a twist defect, and we demonstrate the existence of unconstrained modes which we call supermodes.

As shown schematically in Fig. 1, the filter is formed by a pair of identical chiral mirrors each with N structural half-turns and with a structural angle ξ between them. Additionally, the mirrors are separated by a central isotropic layer defect with refractive index n and thickness d. In our discussion we view the filter as a Fabry-Perot resonator for circularly polarized (CP) light. The resonant wavelength (in vacuum) of the filter is designated as the wavelength λ_0^{Br} at the center of the Bragg resonance associated with each mirror. We use as a parameter the phase thickness of the layer defect at the resonant wavelength, $\phi = 2\pi nd/\lambda_0^{\mathrm{Br}}$. Our task is to derive conditions on n, ϕ, ξ, and N for the transmittance of high-quality CP modes.

The basic element of the filter is a chiral mirror with a twisted biaxial structure, and we begin by reviewing the salient properties of such a reflector. Throughout the Letter we assume that the mirror has a left-handed structure, with in-plane principal refractive indexes n_2 and n_3 twisting through the thickness of the mirror with a structural pitch P. As the optical pitch is $P/2$, the resonant wavelength $\lambda_0^{\mathrm{Br}} = n_{\mathrm{av}}P$. For convenience, we work with $n_{\mathrm{av}} = (n_2 + n_3)/2$ and the in-plane linear birefringence $\Delta n = n_3 - n_2$. In the calculations we use the values $\lambda_0^{\mathrm{Br}} = 620$ nm, $n_2 = 1.45$, and $n_3 = 1.55$ so that $n_{\mathrm{av}} = 1.5$ and $\Delta n = 0.1$.

Basically, a left-handed mirror reflects left CP (LCP) light strongly and without change of handedness at the resonant wavelength λ_0^{Br} but is more or less transparent to right CP (RCP) light. However, a small fraction of the incident light suffers change of handedness, and thus four reflection coefficients ρ_{RR}, ρ_{RL}, ρ_{LR}, and ρ_{LL} and four

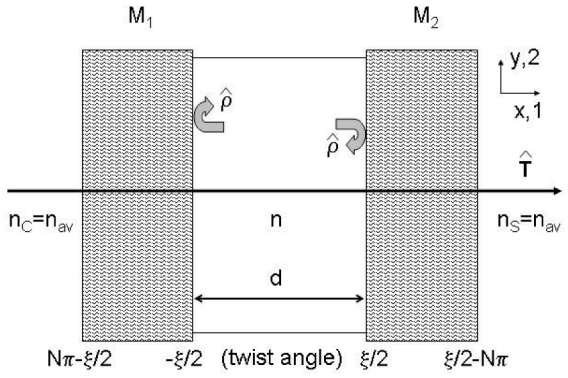

FIG. 1. Left-handed chiral filter with combined layer and twist defects.

transmission coeficients τ_{RR}, τ_{RL}, τ_{LR}, and τ_{LL} are needed to specify the remittance from a chiral mirror. Note that we use subscripts such as RL to indicate RCP out from LCP in, etc. By calculation using a 4×4 field transfer matrix method [8], and from experimental measurements [9], we find that the LL-transmittance spectrum of a typical left-handed mirror is similar to the transmittance spectrum of a dielectric multilayered mirror in that it is characterized by a stop band surrounded by sidebands. Similarly the LL-reflectance spectrum is dominated by a high-reflectance band surrounded by sidebands.

In order to proceed with the Fabry-Perot model of the chiral filter, we consider round-trip propagation in the "spacer" layer, i.e., in the central isotropic layer defect in Fig. 1. For this purpose, we write a 2×2 matrix of amplitude reflection coefficients in the form $\hat{\rho} = [|\rho_{RR}|e^{i\phi_{RR}}e^{-i\xi}, |\rho_{RL}|e^{i\phi_{RL}}; |\rho_{LR}|e^{i\phi_{LR}}, |\rho_{LL}|e^{i\phi_{LL}}e^{i\xi}]$. A simplification can be made because the cross-polarized coefficients are equal; i.e., $|\rho_{RL}|e^{i\phi_{RL}} = |\rho_{LR}|e^{i\phi_{LR}}$. As the mirrors look identical when viewed from inside the layer defect, $\hat{\rho}$ is appropriate to both mirrors. The phase terms in ξ have a simple geometric origin and account for the rotations of the mirrors relative to a standard position, with $\xi = 0$ and principal axis-2 in the plane of Fig. 1 at the internal interface.

Figure 2, which is plotted for $N = 100$, shows typical magnitudes and phases of the elements of the matrix $\hat{\rho}$ for mirrors in the standard position (with $\xi = 0$) and for a range of values of n. Clearly, the upper part of the figure which has a log scale shows that ρ_{LL} is the most significant reflection coefficient, followed by the cross-polarized coefficients ρ_{RL} and ρ_{LR}, and then by ρ_{RR}. The magnitudes of the copolarized coefficients ρ_{RR} and ρ_{LL} are relatively insensitive to the value of n, but the magnitudes of the cross-polarized coefficients decrease significantly when the refractive index n of the layer defect matches the average index n_{av} of the chiral mirrors. The lower part of Fig. 2 shows that ϕ_{RR} and ϕ_{LL} depend weakly on n, in contrast to ϕ_{RL} and ϕ_{LR}. Additional calculations show that the value of N has significant influence only on $|\rho_{RR}|$ ($\approx 10^{-3}$ for $N = 20$) and ϕ_{RR} ($\approx -90°$ for $N = 20$).

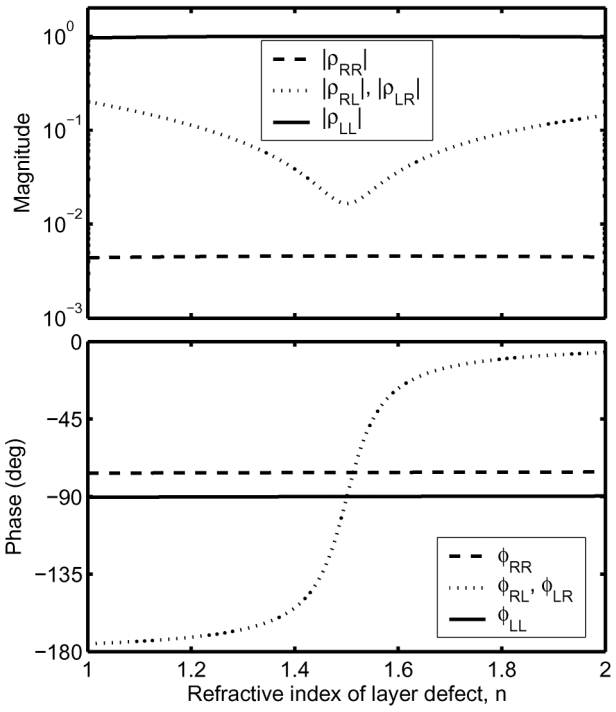

FIG. 2. Magnitudes and phases of the elements of the reflection matrix for chiral mirrors in the standard position ($n_C = n$, $n_S = n_{av} = 1.5$, $N = 100$, $\xi = 0$).

Our basic premise is that a strong resonance will occur if the filter can be tuned so that the elements of the 2×2 round-trip matrix $\hat{X} = \hat{\rho}e^{i\phi}\hat{\rho}e^{i\phi}$ all have the same phase. Then all RR, RL, LR, and LL terms in the Airy summation

$$\hat{I} + \hat{X} + \hat{X}^2 + \hat{X}^3 + \hat{X}^4 \ldots = (\hat{I} - \hat{X})^{-1}, \qquad (1)$$

in which $\hat{I}$ is the 2×2 identity matrix, will be parallel at resonance. Equation (1) essentially provides four phasor diagrams, one each for the RR, RL, LR, and LL terms. In our case, with the chiral mirrors looking the same from within the spacer layer, the phase-matching requirement will be met if the elements of $\hat{\rho}$ all have the same phase. To begin though, we consider resonances acquired by considering just the most significant coefficient, ρ_{LL}. A condition for resonance can then be put in the form $4\pi nd/\lambda_0^{Br} + 2\phi_{LL} + 2\xi = 0$. We are free to choose values of n and d and can determine the approximate tuning angle ξ using

$$\xi = -2\pi nd/\lambda_0^{Br} - \phi_{LL}. \qquad (2)$$

Additional fine-tuning of ξ is necessary in practice, because at this stage we have not controlled the phases of ρ_{RL}, ρ_{LR}, and ρ_{RR}. Figure 3 shows a map of the peak transmittance T_{LL}^{peak} of the central defect mode, computed for CFs with $N = 25$. Two periods are shown — the contours repeat with a period of 180°. The spacerless CF is represented by any point on the lower horizontal axis, where the isotropic layer defect has zero thickness.

The contours corresponding to $T_{LL}^{peak} = 0.25$ partition the map in Fig. 3 into CFs that are below and above the crossover for a saturation effect described by Kopp and Genack for the spacerless CF [6]. Figure 4, which shows the evolution of transmittance line shapes as N is increased, confirms that the same effects of anomalous excitation and saturation of linewidth occur in the general CF with both a layer defect and a twist defect. At the crossover all transmittances and reflectances are approximately equal in our description. If N is increased, the 0.25-transmittance contours move towards the broken-line contours in Fig. 3. For the chosen material values, the spacerless CF reaches the crossover at $N \approx 40$.

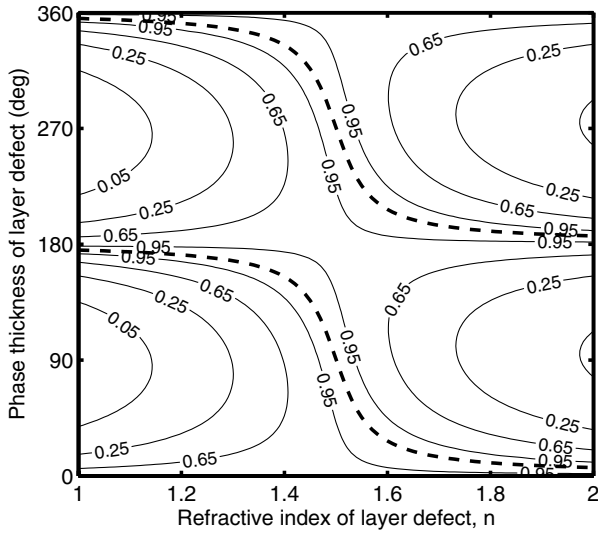

FIG. 3. Peak transmittance $T_{\mathrm{LL}}^{\mathrm{peak}}$ of the central defect mode of CFs ($N = 25$).

Next, we bring about simultaneous resonance of ρ_{RL}, ρ_{LR}, and ρ_{LL} by introducing an additional condition: $\phi_{\mathrm{RL}} = \phi_{\mathrm{LL}} + \xi$. This leads to the equation

$$d = -\phi_{\mathrm{RL}}\lambda_0^{\mathrm{Br}}/2\pi n \tag{3}$$

for the thickness of the layer defect. Hence, the required phase thickness of the layer defect is

$$\phi = -\phi_{\mathrm{RL}}, \tag{4}$$

and the required tuning angle is

$$\xi = \phi_{\mathrm{RL}} - \phi_{\mathrm{LL}}. \tag{5}$$

As before, fine-tuning of ξ is necessary, and the filters are represented by the broken-line contours in Fig. 3.

Our calculations show that the broken-line contours in the map in Fig. 3 remain nearly fixed, and the shape of the basic spectral reflectance and transmittance profiles remain intact, as N is increased from 20 to 100. In general, the designs represented by the broken-line contours are superior in both purity of polarization and spectral linewidth of the transmitted light and would be adequate for most practical applications, but the modes become increasingly difficult to locate with approximate equations as N is increased.

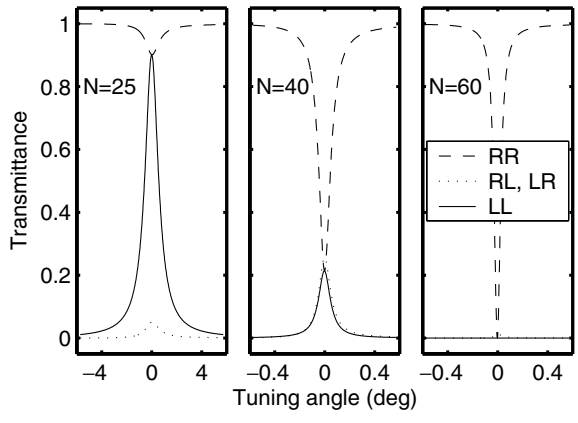

FIG. 4. Anomalous excitation and saturation of spectral linewidth of a CF with a layer defect and a twist defect ($n = 1.6$, $\phi = 54°$).

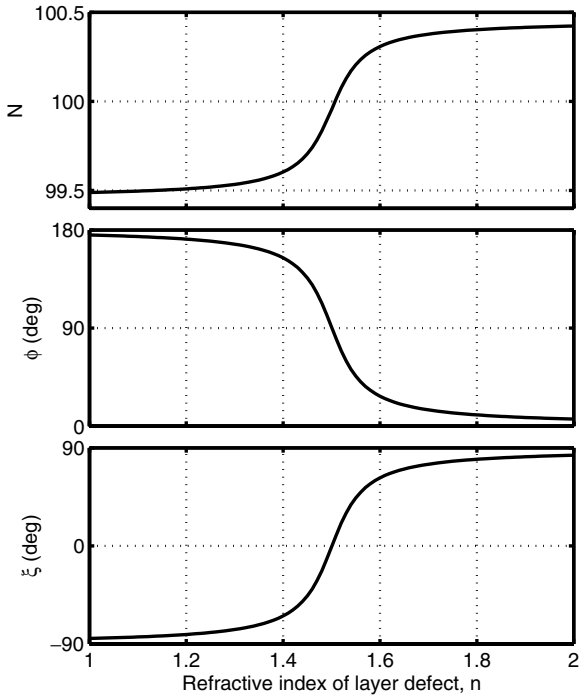

FIG. 5. Parameter values for phase-matched supermodes of CFs with a layer defect and a twist defect.

We continue the discussion by encompassing resonance with the small copolarized coefficient ρ_{RR}. As for the previous resonances, this can be achieved by considering a mirror in the standard position. For a given value of n a fractional part is added to N (which is initially an integer), so that tuning by the total angle ξ defined in Eq. (5) yields $\phi_{\mathrm{RR}} - \xi = \phi_{\mathrm{RL}}$. Hence, a test condition for the final requirement can be framed in terms of the phase change angles of the mirror in the standard position as

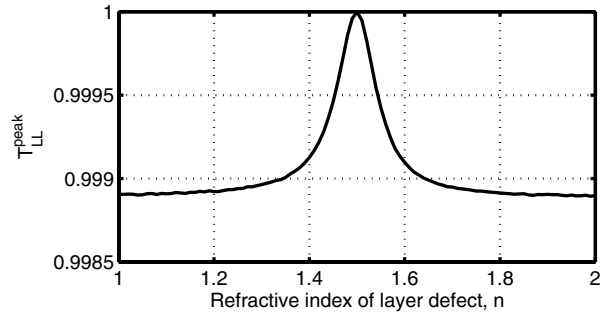

FIG. 6. Peak transmittance of phase-matched supermodes of CFs with a layer defect and a twist defect ($N = 100$).

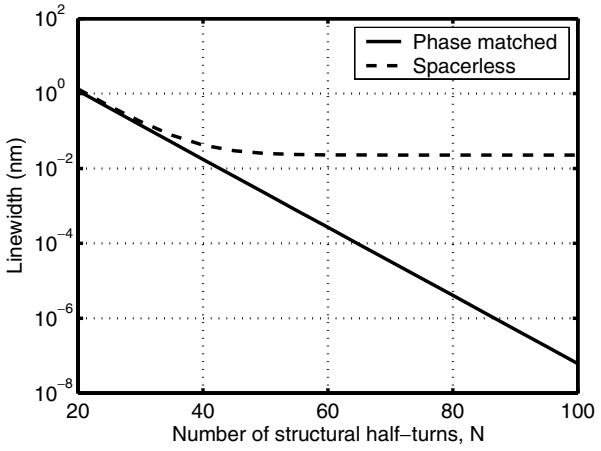

FIG. 7. Solid line: linewidth of phase-matched supermodes of CFs with a layer defect and a twist defect ($n = 1.6$). Broken line: linewidth of saturated modes of spacerless CFs with a 90° twist defect.

$$\phi_{RR} = 2\phi_{RL} - \phi_{LL}. \quad (6)$$

In practice, the fractional N that satisfies Eq. (6) is found by an iterative method as the first step of the entire procedure. Then ϕ and ξ are calculated directly using Eqs. (4) and (5), respectively. Parameter sets $\{n, \phi, \xi, N\}$ that were determined in this way are plotted in Fig. 5. We find that they allow the supermodes to be located without additional fine-tuning. For example, a parameter set determined for $N \approx 100$ positions the supermode at λ_0^{Br} to within a small fraction of the linewidth of 6×10^{-8} nm.

The peak transmittance of the phase-matched supermodes is typically > 0.998 for $1 \leq n \leq 2$, as shown in Fig. 6 for $N = 100$. The solid line in Fig. 7 shows that the computed linewidth of the phase-matched supermodes decreases exponentially as N is increased from 20 to 100. For comparison, we have plotted the linewidth of the defect modes of spacerless filters using a broken line. Clearly, the phase-matched supermodes are not influenced by the effects of anomalous excitation and saturation of linewidth that constrain other designs.

Finally, we note that the weak dependence of the resonance on the value of N allows further tuning of the filter to optimize a property such as the peak tranmittance T_{LL}^{peak}, as suggested by Yang *et al.* [10].

In summary, we have presented a survey of chiral filters with combined central layer and twist defects. The general CF is shown to suffer from the effects of anomalous excitation and saturation of linewidth that are known to constrain the performance of the spacerless CF. However, for each possible value of the refractive index of the layer defect, the general CF can be tuned to a supermode that maintains exceptional purity of the polarization state and an exponential decrease in the linewidth as the number of turns is increased.

The University of Otago authors acknowledge support from the New Zealand New Economy Research Fund and from the MacDiarmid Centre for Research Excellence. A. L. thanks the Trustees of the Pennsylvania State University for support.

*Electronic address: ijh@physics.otago.ac.nz
†Electronic address: qihong@physics.otago.ac.nz
‡Electronic address: ldesilva@physics.otago.ac.nz
§Electronic address: marnold@physics.otago.ac.nz
‖Electronic address: m.mccall@ic.ac.uk
¶Electronic address: AXL4@psu.edu

[1] K. Robbie, M. J. Brett, and A. Lakhtakia, Nature (London) **384**, 616 (1996).
[2] V. I. Kopp, B. Fan, H. K. M. Vithana, and A. Z. Genack, Opt. Lett. **23**, 1707 (1998).
[3] J. Schmidtke, W. Stille, and H. Finkelmann, Phys. Rev. Lett. **90**, 83902 (2003).
[4] I. J. Hodgkinson, Q. h. Wu, A. Lakhtakia, and M.W. McCall, Opt. Commun. **177**, 79 (2000).
[5] I. J. Hodgkinson, Q. H. Wu, K. E. Thorn, A. Lakhtakia, and M.W. McCall, Opt. Commun. **184**, 57 (2000).
[6] V. I. Kopp and A. Z. Genack, Phys. Rev. Lett. **89**, 033901 (2002).
[7] F. Wang and A. Lakhtakia, Opt. Commun. **215**, 79 (2003).
[8] I. J. Hodgkinson, Q. h. Wu, M. Arnold, M.W. McCall, and A. Lakhtakia, Opt. Commun. **210**, 201 (2002).
[9] Q. Wu, I. J. Hodgkinson, and A. Lakhtakia, Opt. Eng. (Bellingham, Wash.) **39**, 1863 (2000).
[10] Y.-C. Yang, C.-S. Kee, J.-E. Kim, and H. Y. Park, Phys. Rev. E **60**, 6852 (1999).